ACS Photonics

Letter

Cite This: ACS Photonics XXXX, XXX, XXX−XXX

pubs.acs.org/journal/apchd5

Drift-Induced Unidirectional Graphene Plasmons

Tiago A. Morgado*,† and Mário G. Silveirinha*,†,‡

†Instituto de Telecomunicações and Department of Electrical Engineering, University of Coimbra, 3030-290 Coimbra, Portugal

‡University of Lisbon, Instituto Superior Técnico, Avenida Rovisco Pais, 1, 1049-001 Lisboa, Portugal

Supporting Information

ABSTRACT: Nonreciprocal photonic devices enable "one-way" light flows and are essential building blocks of optical systems. Here, we investigate an alternative paradigm to break reciprocity and achieve unidirectional subwavelength light propagation fully compatible with modern all-photonic highly integrated systems. In agreement with a few recent studies, our theoretical model predicts that a graphene sheet biased with a drift electric current has a strong nonreciprocal tunable response. Strikingly, we find that the propagation of the surface plasmon polaritons can be effectively "one-way" and may be largely immune to the backscattering from defects and obstacles. Furthermore, the drift-current biasing may boost the propagation length of the graphene plasmons by more than 100%. Our findings open new inroads in nonreciprocal photonics and offer a new opportunity to control the flow of light with one-atom thick nonreciprocal devices.

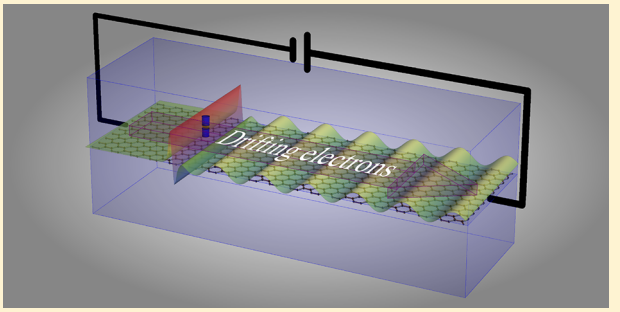

KEYWORDS: *plasmonics, nanophotonics, graphene, nonreciprocal photonics, optical isolation, unidirectional propagation*

Light propagation in conventional photonic systems is constrained by the Lorentz reciprocity law. This fundamental principle is intimately related to the invariance of Maxwell's equations under time-reversal symmetry,[1] which forbids one-way light flows in standard metal-dielectric platforms. According to the reciprocity principle,[2,3] if the positions of the source and receiver are interchanged, the level of the received signal remains the same. Thus, reciprocal systems are inherently bidirectional.

With the ever-increasing demand for all-photonic highly integrated systems,[4] there has been recently a tremendous effort in the development of solutions that permit nonreciprocal light propagation. The standard way to break the Lorentz reciprocity principle is by using a static magnetic field bias that creates a gyrotropic nonreciprocal response.[5−10] In particular, it was recently demonstrated that some gyrotropic material platforms are intrinsically topological and, thereby, may support unidirectional scattering-immune edge states.[11−20] However, the need of an external magnetic biasing hinders the integration of such components in nanophotonic systems. Furthermore, the gyrotropic response is usually rather weak at optics because, for a realistic magnetic bias strength, the cyclotron frequency typically lies in the microwave range. Transistor-loaded metamaterials provide a viable path to create a strong nonreciprocal response with no static magnetic fields, but only at microwave and millimeter-wave frequencies.[21,22]

Alternative solutions to obtain asymmetric light flows have been extensively investigated, namely, by exploiting nonlinear effects[23−27] and opto-mechanical interactions.[28−31] Nevertheless, the requirement of high power signals in nonlinear systems and the typically weak response of opto-mechanical resonators limit the applicability of these solutions. Spatio-temporally modulated waveguides also offer interesting conceptual opportunities to break the reciprocity of light propagation, but these approaches may be difficult to implement and integrate in nanophotonic systems.[32−36]

In this Letter, we explore a simple and innovative platform that provides magnetic-free nonreciprocal subwavelength light propagation through the biasing of a graphene sheet with a drift electric current (Figure 1). Even though the electric drift current bias is a well-established solution to break the Lorentz reciprocity,[37,38] it received only marginal attention in the recent literature because significant nonreciprocal effects require large drift velocities, which are impracticable in metals and in most semiconductors. Here, we highlight that graphene

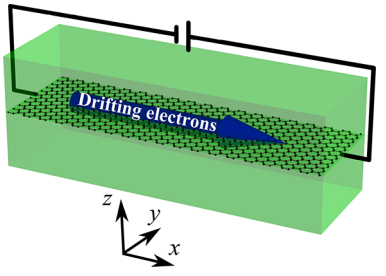

Figure 1. Drift current biasing of graphene. A static voltage generator induces an electron drift in a graphene sheet embedded in a dielectric with relative permittivity $\varepsilon_{r,s} = 4$.

Received: July 19, 2018
Published: October 23, 2018

DOI: 10.1021/acsphotonics.8b00987
ACS Photonics XXXX, XXX, XXX−XXX

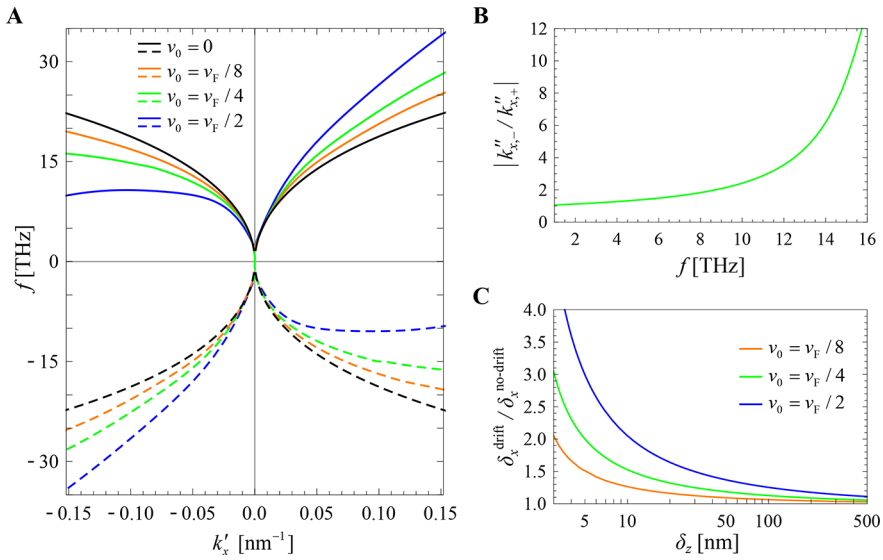

Figure 2. SPPs dispersion diagram. (A) Dispersion of the SPPs supported by the graphene sheet for different drift velocities v_0 and for both positive and negative frequencies. (B) Ratio between the imaginary parts of the guided wave numbers of the drift-induced SPPs that propagate along the $-x$ and $+x$ directions as a function of the frequency for a drift velocity $v_0 = v_F/4$. (C) Ratio between the SPP propagation lengths (δ_x) with and without drift-current biasing as a function of the SPP lateral decay length (δ_z) for the forward SPP (propagating along $+x$; the SPP dispersion is depicted with a solid line in panel A).

may offer a truly unique opportunity in this context: it has an ultrahigh electron mobility and enables drift velocities on the order of $c/300$,[39−43] which may be several orders of magnitude larger than in typical metals[38] and several times larger than in high-mobility semiconductors.[44,45] Motivated by these properties, we theoretically show that the high electron mobility of graphene can enable a broadband subwavelength "one-way" propagation regime and waveguiding immune to backscattering due to the presence of near-field scatterers or other structural imperfections. Remarkably, the drift-current biasing can change the graphene conductivity dispersion and boost the propagation length of the graphene plasmons.

A few recent works studied the impact of an electric current bias in the graphene response in different contexts,[46−50] but the possibility of waveguiding immune to back-reflections in graphene was not discussed. The drift current bias was taken into account in refs 46−48 through a semiclassical correction of the equilibrium distribution of the electrons in graphene, but its effect on the energy dispersion and wave functions of the electronic states was neglected. In contrast, the conductivity model adopted in the present study is obtained using purely quantum mechanical methods (self-consistent field approach; see the Supporting Information of ref 50). The effect of the drift current is described by an approximate interaction Hamiltonian of the form $\hat{H}_{int,drift} = \mathbf{v}_0 \cdot \hat{\mathbf{p}}$ ($\hat{\mathbf{p}} = -i\hbar\nabla$ is the momentum operator), which shifts the electrons velocity by $\mathbf{v}_0$. This interaction Hamiltonian neglects the dependence of the drift velocity on the electron energy. Different from the theory of refs 46−48, our approach predicts the frequency Doppler shift due to the motion of the drifting electrons and hence stronger nonreciprocal effects. We would like to underscore that a drift current bias is fundamentally different from the standard electrical tuning of the graphene response through the control of the Fermi level, see, for example, refs 51 and 52.

RESULTS AND DISCUSSION

To begin with, we investigate the propagation of the SPPs supported by a graphene sheet traversed by a DC electric current supplied by a voltage generator. In the absence of a drift current, the graphene sheet is characterized by a surface conductivity $\sigma_g(\omega)$, which is described by the Kubo formula and takes into account both intraband and interband transitions.[53−55] We assume throughout this manuscript that the chemical potential of the graphene sheet is $\mu_c = 0.1$ eV, $T = 300$ K (i.e., room temperature), and that the intraband and interband scattering rates are $\Gamma_{intra} = 1/(0.35\text{ ps})$ and $\gamma_{inter} = 1/(0.0658\text{ ps})$, respectively.[54] The graphene sheet is surrounded by a dielectric (SiO_2 or h-BN). Moreover, it is assumed that the time variation is of the form $e^{-i\omega t}$, where ω is the oscillation frequency. For simplicity, here we neglect the intrinsic nonlocal response of graphene[55,56] ($\sigma_g = \sigma_g(\omega,k_x)$), but its impact on the SPP propagation is analyzed in the Supporting Information for low temperatures.

Recently, it was demonstrated by us[50] using the self-consistent field approach that in the presence of drifting electrons with velocity $\mathbf{v}=v_0\hat{\mathbf{x}}$ the graphene conductivity associated with a longitudinal excitation (with in-plane electric field directed along x) is of the form $\sigma_g^{drift}(\omega,k_x) = (\omega/\tilde{\omega})\sigma_g(\tilde{\omega})$, where $\tilde{\omega} = \omega - k_x v_0$ is the Doppler-shifted frequency and k_x is the wavenumber along the x-direction. Interestingly, this result implies that with the drift current (i.e., for $v_0 \neq 0$) $\sigma_g^{drift}(\omega,k_x) \neq \sigma_g^{drift}(\omega,-k_x)$, and thereby, the electromagnetic response of the graphene sheet is nonreciprocal.[57] Note that the time-reversal operation flips the drift velocity, and thus, the response of the graphene sheet with a drift current is not time-reversal invariant.[1] It is worth mentioning that temperature gradients can also create drift currents and, thereby, offer a different mechanism to break the reciprocity of graphene.

To study the opportunities created by the drift current biasing, next we characterize the graphene plasmons. By solving Maxwell's equations, it can be shown that the dispersion characteristic of the SPPs supported by a graphene sheet is determined by $\frac{2}{\gamma_s} i\omega\varepsilon_0\varepsilon_{r,s} - \sigma_g^{drift} = 0$,[55] where c is the speed of light in vacuum, $\varepsilon_0\varepsilon_{r,s}$ is the permittivity of the dielectric substrate, and $\gamma_s = \sqrt{k_x^2 - \varepsilon_{r,s}(\omega/c)^2}$ is the trans-

DOI: 10.1021/acsphotonics.8b00987
ACS Photonics XXXX, XXX, XXX−XXX

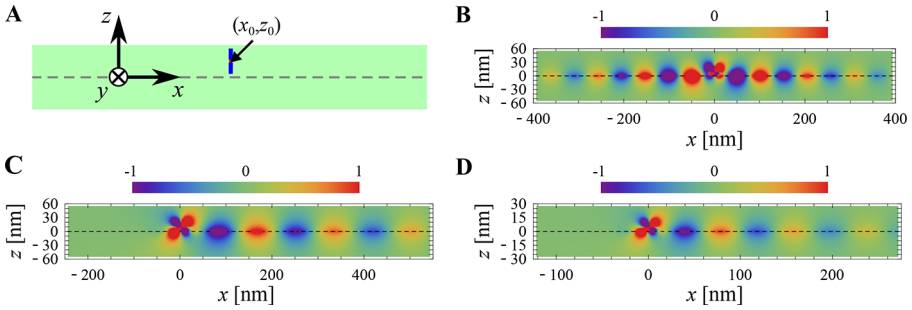

Figure 3. SPP excitation by a near-field emitter. (A) A linearly polarized emitter (with vertical polarization) is placed near the graphene sheet at (x, z) = (0, z_0). (B–D) Time snapshots of the x-component of the electric field E_x (in arbitrary unities). (B) Without a drift current bias. (C, D) With a drift current bias. (B) $v_0 = 0$, $z_0 = 10$ nm, and $f = 15$ THz; (C) $v_0 = v_F/2$, $z_0 = 10$ nm, and $f = 15$ THz; (D) $v_0 = v_F/4$, $z_0 = 5$ nm, and $f = 20$ THz.

verse (along z) attenuation constant that determines the confinement of the graphene plasmons. Evidently, without the drift current, the same formula holds with σ_g^{drift} replaced by σ_g.

Figure 2A depicts the dispersion characteristic of the SPPs for different drift velocities v_0. For clarity, we represent both the positive and the negative frequency solutions. The reality of the electromagnetic field implies that the positive and negative frequency solutions are mapped one into another as $\omega(k_x) \rightarrow -\omega(-k_x^*)$ (particle hole-symmetry). Because of the graphene absorption, the guided wavenumber of the SPPs is typically complex-valued, $k_x = k_x' + ik_x''$. In the absence of the drift-current ($v_0 = 0$), the ω versus k_x dispersion curve is formed by two symmetric branches (black solid and dashed curves in Figure 2A) corresponding to two counter-propagating waves. The two positive frequency branches are linked by $\omega(k_x') = \omega(-k_x')$, in agreement with the reciprocity and parity symmetries of the system. In contrast, with the drift current biasing, there is an evident symmetry breaking of the SPPs dispersion such that the $+x$ and $-x$ directions become inequivalent. The asymmetry of the dispersion curve is more pronounced when the drift velocity increases. A similar but weaker effect was predicted in refs 46–48. A detailed comparison between our findings and previous work is reported in the Supporting Information. Notably, the symmetry breaking gives rise to a wide frequency range, wherein the SPPs are allowed to propagate along the $+x$ direction (the direction of the drift velocity) but are forbidden (or strongly attenuated) in the opposite direction. For instance, for a drift velocity $v_0 = v_F/2$ ($v_F \approx c/300$ is the Fermi velocity), a regime of unidirectional propagation along the $+x$ direction emerges for frequencies above 10 THz (see the blue solid curves of Figure 2A). Even though the drift velocity in graphene can be on the order of the Fermi velocity,[39−43] it is interesting to see from Figure 2A that the one-way propagation regime may be attainable for drift velocities as low as $v_0 = v_F/8$. Furthermore, as illustrated in Figure 2B, the graphene plasmons that propagate along the negative x-direction are more strongly affected by dissipation than plasmons that propagate along the positive x-direction. The inclusion of nonlocal corrections in the graphene response weakens somewhat the nonreciprocal response, but does not change the unidirectional character of the plasmons (see the Supporting Information), namely, the discrepancy between the attenuation constants $|k_x''|$ of counter-propagating graphene plasmons. Nonlocal effects are stronger when $|k_x'|$ is comparable to or larger than the Fermi wavenumber $k_F = \mu_c/(\hbar v_F)$ ($k_F = 0.15$ nm^{-1} in Figure 2; see the Supporting Information), but such a region is not interesting for waveguiding applications due to the relatively short propagation distance of short-wavelength SPPs.

To further characterize the properties of the graphene plasmons with a drift-current biasing, we calculated the propagation length $\delta_x = 1/\mathrm{Im}\{k_x\}$ as a function of the lateral decay length $\delta_z = 1/\mathrm{Re}\{\gamma_s\}$. Figure 2C shows the ratio between the SPP propagation lengths ($\delta_x^{drift}/\delta_x^{no\text{-}drift}$) with and without a drift-current biasing for the $k_x' > 0$ branch represented with solid lines in Figure 2A. Remarkably, the propagation length of the SPPs with the drift current may significantly exceed that of the SPPs in the absence of a bias current. For example, for $v_0 = v_F/2$ and $\delta_z = 10$ nm, the distance traveled by the SPP wave is twice as large as for the case without biasing. Indeed, for the lateral confinement $\delta_z = 10$ nm, the SPP propagation length is $\delta_x = 174$ nm for $v_0 = v_F/2$, whereas in the absence of a bias current, the propagation length is only $\delta_x = 85$ nm. The increased propagation length of the SPPs stems from the Doppler shift undergone by the graphene conductivity due to the drifting electrons, which changes the material dispersion and weakens the dissipation effects. It should be noted that due to the drift-current bias our system has an "active" response,[50] which may play some role in the enhanced propagation length. Unlike the bilayer graphene system considered in ref 50, the configuration under study does not support electromagnetic instabilities and spasing because such an effect requires the interaction of two surface modes.

To further highlight the emergence of a one-way propagation regime in the drift-current biased graphene, next we consider a scenario wherein the plasmons are excited by a linearly polarized emitter placed in the close proximity of the graphene sheet (Figure 3A). The radiated and scattered electromagnetic fields are calculated using the formalism described in the Supporting Information. Figures 3B-D show time snapshots of the longitudinal component of the electric field (E_x) excited by the near field of the emitter. In the first example (Figure 3B), it is assumed that there is no drift current. Clearly, in this case the wave propagation is bidirectional and two identical counter-propagating SPPs are excited by the emitter (see Figure 3B). Quite differently, when a biasing DC current is used, the response of the system becomes strongly nonreciprocal and the SPPs are "dragged" by the drifting electrons so that they can propagate only along the $+x$ direction (see Figure 3C,D), in agreement with Figure 2A. Qualitatively similar results are obtained when the nonlocality of the bare graphene response is taken into account (see the Supporting Information).

Here, we note that other works have previously demonstrated the excitation of directive plasmons in graphene.[58−61]

DOI: 10.1021/acsphotonics.8b00987
ACS Photonics XXXX, XXX, XXX−XXX

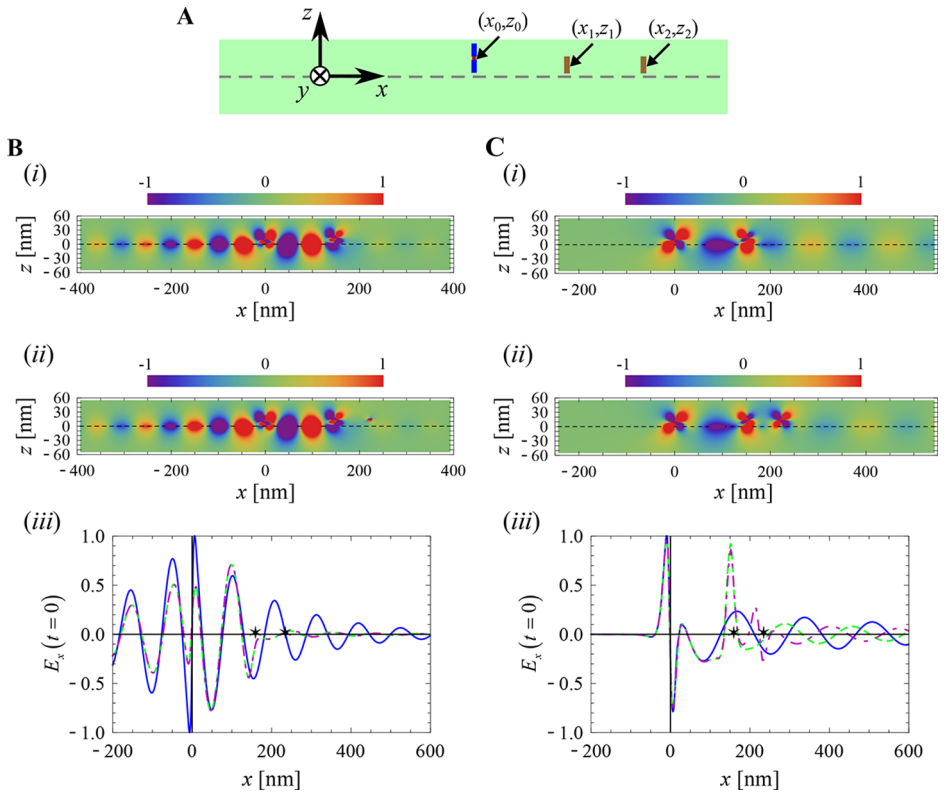

Figure 4. SPP propagation with obstacles. (A) A linearly polarized emitter and thin strip obstacles are placed near the graphene sheet. (B, C) Similar to Figure 3B,C, but with one or more obstacles at the positions (x_i, z_i). (B) Without a drift current bias. (C) With a drift current bias with $v_0 = v_F/2$. (B*i*, C*i*) With a single obstacle at $(x_1, z_1) = (150\text{ nm}, 15\text{ nm})$; (B*ii*, C*ii*) With two obstacles at $(x_1, z_1) = (150\text{ nm}, 15\text{ nm})$ and $(x_2, z_2) = (225\text{ nm}, 15\text{ nm})$. (B*iii*, C*iii*) Snapshots in time of E_x (in arbitrary unities) as a function of x and for $z = 0$. Blue solid lines: without obstacles; green dashed lines: with a single obstacle; purple dot-dashed lines: with the two obstacles. The two black stars in (B*iii*, C*iii*) represent the position of the obstacles; the emitter is at the origin.

However, such proposals rely on asymmetric excitations of the SPPs, for example, by using gratings[58−60] or emitters with circular polarization.[61] These solutions are fully reciprocal, and hence, the graphene plasmons are bidirectional. In contrast, our system is genuinely "one-way" and, thereby, independently of the excitation or of the polarization of the emitter, the plasmons are launched toward the $+x$-direction.

The "one-way" property implies that the graphene plasmons cannot be backscattered by an obstacle or defect, somewhat similar to topological structures.[6,11−15] In our system, the dielectric is a transparent material. Hence, in principle, the plasmons may be scattered by an obstacle as plane-wave states of the dielectric, even though for near-field interactions such a process is inefficient. Moreover, since graphene is a lossy material, part of the energy transported by the plasmon may be dissipated near the obstacle. To illustrate these ideas, next we study how the presence of scatterers affects the SPP propagation. We consider a setup similar to that of Figure 3A, except that one or more metallic strips are placed along the SPPs propagation path (see Figure 4A). For simplicity, all the obstacles are characterized by the same relative permittivity ($\varepsilon_{r,i} = -4.1$) and by the same width ($w_i = 12$ nm). To determine the influence of the objects on the wave propagation we use the formalism described in the Supporting Information, which treats the obstacles as secondary sources of radiation.

The calculated time snapshots of the x-component of the electric field are depicted in Figure 4B,C. Without a drift current, the propagation is bidirectional, and for this reason the obstacles strongly backscatter the SPP mode (see Figure 4B*i*,*ii*). Quite differently, with a biasing drift current (Figure 4C*i*,*ii*), there is no backward channel of propagation (i.e., along $-x$ direction) and, hence, no back-reflection is observed. In this case, the plasmons are forced to go around the obstacles and a strong transmission level is observed. As previously noted, part of the energy of the plasmons may be dissipated at the obstacles or leak into the bulk dielectric. From the density plots, the latter process appears to be of secondary importance.

The backscattering suppression is even more evident from the results of Figure 4B*iii*,C*iii*, where E_x is depicted as a function of x and for $z = 0$. As seen, when the graphene sheet is under a DC current biasing (Figure 4C*iii*), the field before the obstacles is unperturbed, even when the propagation path is obstructed by two scatterers (purple dot-dashed curve in Figure 4C*iii*). On the other hand, beyond obstacles position, the field amplitude is almost the same as when the propagation path is free. The slight amplitude reduction is mainly due to material absorption. In contrast, without the bias drift current (Figure 4B*iii*), the forward SPP is back-reflected so strongly by the obstacles that it practically vanishes beyond the obstacles positions. A more detailed analysis of the influence of the obstacles on the transmitted field is given in the Supporting Information.

CONCLUSIONS

In summary, we have shown that a drift current breaks the reciprocal response of the graphene conductivity and enables a broadband regime of "one-way" SPP propagation. The proposed one-atom thick nonreciprocal platform has a tunable

DOI: 10.1021/acsphotonics.8b00987
ACS Photonics XXXX, XXX, XXX−XXX

and switchable response: the graphene conductivity can be controlled either by changing the drift velocity or the chemical potential. Furthermore, the direction of propagation of the unidirectional plasmons is determined by the sign of the drift velocity. Importantly, the drift-current biasing enhances the propagation length of the graphene SPPs by factors of up to 2−4. The unidirectional SPPs are protected against back-scattering from obstacles and defects, analogous to topological systems. The proposed system can be used as a building block of a wide range of nonreciprocal circuits, for example, optical isolators and circulators. Thus, our findings open up a new and exciting route to control the flow of light in highly integrated nonreciprocal tunable nanophotonic circuits.

■ ASSOCIATED CONTENT

Supporting Information

The Supporting Information is available free of charge on the ACS Publications website at DOI: 10.1021/acsphotonics.8b00987.

(A) The comparison of our theory with other results from the literature and the analysis of the impact of nonlocal effects; (B) Derivation of the plane-wave reflection and transmission coefficients for a drift-current biased graphene sheet; (C, D) Derivation of the fields radiated by a linearly polarized emitter placed near the drift-current biased graphene without and with scattering obstacles, respectively; (E) Study of the attenuation caused by the interaction of an obstacle with the SPP wave (PDF).

■ AUTHOR INFORMATION

Corresponding Authors

*E-mail: tiago.morgado@co.it.pt.
*E-mail: mario.silveirinha@co.it.pt.

ORCID

Tiago A. Morgado: 0000-0002-8500-9885
Mário G. Silveirinha: 0000-0002-3730-1689

Notes

The authors declare no competing financial interest.

■ ACKNOWLEDGMENTS

This work was partially funded by Fundação para a Ciência e a Tecnologia PTDC/EEI-TEL/4543/2014 and by Instituto de Telecomunicações under Project UID/EEA/50008/2017. T.A.M. acknowledges financial support by Fundação para a Ciência e a Tecnologia (FCT/POPH) and the cofinancing of Fundo Social Europeu under the Post-Doctoral Fellowship SFRH/BPD/84467/2012.

■ REFERENCES

(1) Casimir, H. B. G. On Onsager's principle of microscopic reversibility. *Rev. Mod. Phys.* **1945**, *17*, 343−350.
(2) Potton, R. J. Reciprocity in optics. *Rep. Prog. Phys.* **2004**, *67*, 717−754.
(3) Deák, L.; Fülöp, T. Reciprocity in quantum, electromagnetic and other wave scattering. *Ann. Phys.* **2012**, *327*, 1050−1077.
(4) Koenderink, A. F.; Alù, A.; Polman, A. Nanophotonics: Shrinking light-based technology. *Science* **2015**, *348*, 516−521.
(5) Wang, Z.; Fan, S. Optical circulators in two-dimensional magneto-optical photonic crystals. *Opt. Lett.* **2005**, *30*, 1989−1991.
(6) Yu, Z.; Veronis, G.; Wang, Z.; Fan, S. One-Way Electromagnetic Waveguide Formed at the Interface between a Plasmonic Metal under a Static Magnetic Field and a Photonic Crystal. *Phys. Rev. Lett.* **2008**, *100*, 023902.
(7) Wang, Z.; Chong, Y. D.; Joannopoulos, J. D.; Soljačić, M. Reflection-Free One-Way Edge Modes in a Gyromagnetic Photonic Crystal. *Phys. Rev. Lett.* **2008**, *100*, 013905.
(8) Davoyan, A. R.; Engheta, N. Theory of Wave Propagation in Magnetized Near-Zero-Epsilon Metamaterials: Evidence of One-Way Photonic States and Magnetically Switched Transparency and Opacity. *Phys. Rev. Lett.* **2013**, *111*, 257401.
(9) Lin, X.; Xu, Y.; Zhang, B.; Hao, R.; Chen, H.; Li, E. Unidirectional surface plasmons in nonreciprocal graphene. *New J. Phys.* **2013**, *15*, 113003.
(10) Prudêncio, F. R.; Silveirinha, M. G. Optical isolation of circularly polarized light with a spontaneous magnetoelectric effect. *Phys. Rev. A: At., Mol., Opt. Phys.* **2016**, *93*, 043846.
(11) Lu, L.; Joannopoulos, J. D.; Soljačić, M. Topological photonics. *Nat. Photonics* **2014**, *8*, 821−829.
(12) Lu, L.; Joannopoulos, J. D.; Soljačić, M. Topological states in photonic systems. *Nat. Phys.* **2016**, *12*, 626−629.
(13) Haldane, F. D. M.; Raghu, S. Possible realization of directional optical waveguides in photonic crystals with broken time-reversal symmetry. *Phys. Rev. Lett.* **2008**, *100*, 013904.
(14) Raghu, S.; Haldane, F. D. M. Analogs of quantum-Hall-effect edge states in photonic crystals. *Phys. Rev. A: At., Mol., Opt. Phys.* **2008**, *78*, 033834.
(15) Wang, Z.; Chong, Y.; Joannopoulos, J. D.; Soljačić, M. Observation of unidirectional backscattering-immune topological electromagnetic states. *Nature* **2009**, *461*, 772−775.
(16) Poo, Y.; Wu, R.-X.; Lin, Z.; Yang, Y.; Chan, C. T. Experimental Realization of Self-Guiding Unidirectional Electromagnetic Edge States. *Phys. Rev. Lett.* **2011**, *106*, 093903.
(17) Jacobs, D. A.; Miroshnichenko, A. E.; Kivshar, Y. S.; Khanikaev, A. B. Photonic topological Chern insulators based on Tellegen metacrystals. *New J. Phys.* **2015**, *17*, 125015.
(18) Silveirinha, M. G. Chern Invariants for Continuous Media. *Phys. Rev. B: Condens. Matter Mater. Phys.* **2015**, *92*, 125153.
(19) Silveirinha, M. G. Bulk edge correspondence for topological photonic continua. *Phys. Rev. B: Condens. Matter Mater. Phys.* **2016**, *94*, 205105.
(20) Silveirinha, M. G. PTD Symmetry Protected Scattering Anomaly in Optics. *Phys. Rev. B: Condens. Matter Mater. Phys.* **2017**, *95*, 035153.
(21) Kodera, T.; Sounas, D. L.; Caloz, C. Artificial Faraday rotation using a ring metamaterial structure without static magnetic field. *Appl. Phys. Lett.* **2011**, *99*, 031114.
(22) Wang, Z.; Wang, Z.; Wang, J.; Zhang, B.; Huangfu, J.; Joannopoulos, J. D.; Soljačić, M.; Ran, L. Gyrotropic response in absence of a bias field. *Proc. Natl. Acad. Sci. U. S. A.* **2012**, *109*, 13194−13197.
(23) Gallo, K.; Assanto, G.; Parameswaran, K. R.; Fejer, M. M. All-optical diode in a periodically poled lithium niobate waveguide. *Appl. Phys. Lett.* **2001**, *79*, 314−316.
(24) Soljačić, M.; Luo, C.; Joannopoulos, J. D.; Fan, S. Nonlinear photonic crystal microdevices for optical integration. *Opt. Lett.* **2003**, *28*, 637−639.
(25) Ramezani, H.; Kottos, T.; El-Ganainy, R.; Christodoulides, D. N. Unidirectional nonlinear PT-symmetric optical structures. *Phys. Rev. A: At., Mol., Opt. Phys.* **2010**, *82*, 043803.
(26) Shadrivov, I. V.; Fedotov, V. A.; Powell, D. A.; Kivshar, Y. S.; Zheludev, N. I. Electromagnetic wave analogue of an electronic diode. *New J. Phys.* **2011**, *13*, 033025.
(27) Fan, L.; Wang, J.; Varhese, L. T.; Shen, H.; Niu, B.; Xuan, Y.; Weiner, A. M.; Qi, M. An all-silicon passive optical diode. *Science* **2012**, *335*, 447−450.
(28) Weiss, S.; Rivière, R.; Deléglise, S.; Gavartin, E.; Arcizet, O.; Schliesser, A.; Kippenberg, T. J. Optomechanically induced transparency. *Science* **2010**, *330*, 1520−1523.
(29) Hafezi, M.; Rabl, P. Optomechanically induced non-reciprocity in microring resonators. *Opt. Express* **2012**, *20*, 7672−7684.

DOI: 10.1021/acsphotonics.8b00987
ACS Photonics XXXX, XXX, XXX−XXX

(30) Fleury, R.; Sounas, D. L.; Sieck, C. F.; Haberman, M. R.; Alù, A. Sound Isolation and Giant Linear Nonreciprocity in a Compact Acoustic Circulator. *Science* **2014**, *343*, 516−519.
(31) Lannebère, S.; Silveirinha, M. G. Wave instabilities and unidirectional light flow in a cavity with rotating walls. *Phys. Rev. A: At., Mol., Opt. Phys.* **2016**, *94*, 033810.
(32) Yu, Z.; Fan, S. Complete optical isolation created by indirect interband photonic transitions. *Nat. Photonics* **2009**, *3*, 91−94.
(33) Lira, H.; Yu, Z.; Fan, S.; Lipson, M. Electrically driven nonreciprocity induced by interband photonic transition on a silicon chip. *Phys. Rev. Lett.* **2012**, *109*, 033901.
(34) Sounas, D. L.; Caloz, C.; Alù, A. Giant non-reciprocity at the subwavelength scale using angular momentum-biased metamaterials. *Nat. Commun.* **2013**, *4*, 2407.
(35) Sounas, D. L.; Alù, A. Angular-momentum-biased nanorings to realize magnetic-free integrated optical isolation. *ACS Photonics* **2014**, *1*, 198−204.
(36) Estep, N. A.; Sounas, D. L.; Soric, J.; Alù, A. Magnetic-free non-reciprocity and isolation based on parametrically modulated coupled-resonator loops. *Nat. Phys.* **2014**, *10*, 923−927.
(37) Davoyan, A.; Engheta, N. Electrically controlled one-way photon flow in plasmonic nanostructures. *Nat. Commun.* **2014**, *5*, 5250.
(38) Bliokh, K. Y.; Fortuño, F. J. R.; Bekshaev, A. Y.; Kivshar, Y. S.; Nori, F. Electric current induced unidirectional propagation of surface plasmon-polaritons. *Opt. Lett.* **2018**, *43*, 963−966.
(39) Shishir, R. S.; Ferry, D. K. Velocity saturation in intrinsic graphene. *J. Phys.: Condens. Matter* **2009**, *21*, 344201.
(40) Dorgan, V. E.; Bae, M.-H.; Pop, E. Mobility and saturation velocity in graphene on SiO_2. *Appl. Phys. Lett.* **2010**, *97*, 082112.
(41) Ozdemir, M. D.; Atasever, O.; Ozdemir, B.; Yarar, Z.; Ozdemir, M. A comparative study of transport properties of monolayer graphene and AlGaN-GaN heterostructure. *AIP Adv.* **2015**, *5*, 077101.
(42) Ramamoorthy, H.; Somphonsane, R.; Radice, J.; He, G.; Kwan, C. P.; Bird, J. P. "Freeing" Graphene from Its Substrate: Observing Intrinsic Velocity Saturation with Rapid Electrical Pulsing. *Nano Lett.* **2016**, *16*, 399−403.
(43) Yamoah, M. A.; Yang, W.; Pop, E.; Goldhaber-Gordon, D. High-Velocity Saturation in Graphene Encapsulated by Hexagonal Boron Nitride. *ACS Nano* **2017**, *11*, 9914−9919.
(44) Hrostowski, H. J.; Morin, F. J.; Geballe, T. H.; Wheatley, G. H. Hall effect and conductivity of InSb. *Phys. Rev.* **1955**, *100*, 1672−1676.
(45) Chen, J. H.; Jang, C.; Xiao, S.; Ishigami, M.; Fuhrer, M. S. Intrinsic and Extrinsic Performance Limits of Graphene Devices on SiO_2. *Nat. Nanotechnol.* **2008**, *3*, 206−209.
(46) Van Duppen, B.; Tomadin, A.; Grigorenko, A. N.; Polini, M. Current-induced birefrigent absorption and non-reciprocal plasmons in graphene. *2D Mater.* **2016**, *3*, 015011.
(47) Sabbaghi, M.; Lee, H.-W.; Stauber, T.; Kim, K. S. Drift-induced modifications to the dynamical polarization of graphene. *Phys. Rev. B: Condens. Matter Mater. Phys.* **2015**, *92*, 195429.
(48) Wenger, T.; Viola, G.; Kinaret, J.; Fogelström, M.; Tassin, P. Current-controlled light scattering and asymmetric plasmon propagation in graphene. *Phys. Rev. B: Condens. Matter Mater. Phys.* **2018**, *97*, 085419.
(49) Borgnia, D. S.; Phan, T. V.; Levitov, L. S. Quasi-Relativistic Doppler Effect and Non-Reciprocal Plasmons in Graphene. *arXiv: 1512.09044* **2015**, na.
(50) Morgado, T. A.; Silveirinha, M. G. Negative Landau damping in bilayer graphene. *Phys. Rev. Lett.* **2017**, *119*, 133901.
(51) Qian, H.; Ma, Y.; Yang, Q.; Chen, B.; Liu, Y.; Guo, X.; Lin, S.; Ruan, J.; Liu, X.; Tong, L.; Wang, Z. L. Electrical Tuning of Surface Plasmon Polariton Propagation in Graphene-Nanowire Hybrid Structure. *ACS Nano* **2014**, *8* (3), 2584−2589.
(52) Liu, Y.; Zhang, J.; Liu, H.; Wang, S.; Peng, L.-M. Electrically driven monolithic subwavelength plasmonic interconnect circuits. *Science Adv.* **2017**, *3* (10), e1701456.
(53) Gusynin, V. P.; Sharapov, S. G.; Carbotte, J. P. Magneto-optical conductivity in graphene. *J. Phys.: Condens. Matter* **2007**, *19*, 026222.
(54) Hanson, G. W.; Gangaraj, S. A. H.; Lee, C.; Angelakis, D. G.; Tame, M. Quantum plasmonic excitation in graphene and loss-insensitive propagation. *Phys. Rev. A: At., Mol., Opt. Phys.* **2015**, *92*, 013828.
(55) Gonçalves, P. A. D.; Peres, N. M. R. *An Introduction to Graphene Plasmonics*; World Scientific: Hackensack, NJ, 2016.
(56) Lundeberg, M. B.; Gao, Y.; Asgari, R.; Tan, C.; Van Duppen, B.; Autore, M.; Alonso-González, P.; Woessner, A.; Watanabe, K.; Taniguchi, T.; Hillenbrand, R.; Hone, J.; Polini, M.; Koppens, F. H. L. Tuning quantum nonlocal effects in graphene plasmonics. *Science* **2017**, *357*, 187−191.
(57) Landau, L. D.; Lifshitz, E. M. *Electrodynamics of Continuous Media; Course of Theoretical Physics*; Elsevier Butterworth-Heinemann, 2004; Vol. *8*.
(58) Bonodi, N.; Popov, E.; Chernov, B. Unidirectional excitation of surface plasmons by slanted gratings. *Opt. Express* **2007**, *15*, 11427−11432.
(59) Radko, I. P.; Bolzhevolnyi, S. I.; Brucoli, G.; Martín-Moreno, L.; García-Vidal, F. J.; Boltasseva, A. Efficient unidirectional ridge excitation of surface plasmons. *Opt. Express* **2009**, *17*, 7228−7232.
(60) Li, X.; Tan, Q.; Bai, B.; Jin, G. Experimental demonstration of tunable directional excitation of surface plasmon polaritons with a subwavelength metallic double slit. *Appl. Phys. Lett.* **2011**, *98*, 251109.
(61) Fortuño, F. J. R.; Marino, G.; Ginzburg, P.; O'Connor, D.; Martínez, A.; Wurtz, G. A.; Zayats, A. V. Near-Field Interference for the Unidirectional Excitation of Electromagnetic Guided Modes. *Science* **2013**, *340*, 328−330.

DOI: 10.1021/acsphotonics.8b00987
ACS Photonics XXXX, XXX, XXX−XXX